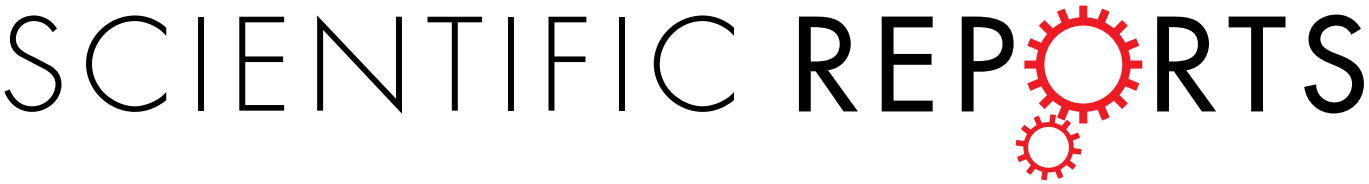

OPEN

Mutual influence between current-induced giant magnetoresistance and radiation-induced magnetoresistance oscillations in the GaAs/AlGaAs 2DES

Received: 15 February 2017
Accepted: 26 May 2017
Published online: 11 July 2017

R. L. Samaraweera[1], H.-C. Liu[1], Z. Wang[1], C. Reichl[2], W. Wegscheider[2] & R. G. Mani[1]

Radiation-induced magnetoresistance oscillations are examined in the GaAs/AlGaAs 2D system in the regime where an observed concurrent giant magnetoresistance is systematically varied with a supplementary dc-current, I_{dc}. The I_{dc} tuned giant magnetoresistance is subsequently separated from the photo-excited oscillatory resistance using a multi-conduction model in order to examine the interplay between the two effects. The results show that the invoked multiconduction model describes the observed giant magnetoresistance effect even in the presence of radiation-induced magnetoresistance oscillations, the magnetoresistance oscillations do not modify the giant magnetoresistance, and the magnetoresistance oscillatory extrema, i.e., maxima and minima, disappear rather asymmetrically with increasing I_{dc}. The results suggest the interpretation that the I_{dc} serves to suppress scattering between states near the Fermi level in a strong magnetic field limit.

The realization of novel photo-excited zero-resistance states and 1/4–cycle shifted magnetoresistance oscillations in the high quality GaAs/AlGaAs two-dimensional electron system by low energy photons in the low magnetic field, high filling factor limit[1–3] has led to new interest in the experimental[1–39] and theoretical[40–62] study of photo-excited transport in low dimensional systems. The same high quality GaAs/AlGaAs two-dimensional electron system (2DES) has also served to provide new insights into an observable giant magnetoresistance in the 2DES[63–81]. Here, for example, recent studies have shown remarkable features such as size dependence and simple tunability of the GMR with a supplemental dc-current (I_{dc})[77,80]. The observability of these two-interesting effects over the same range of magnetic fields and temperatures has created experimental interest into the questions related to the mutual influence between the photo-excited oscillatory magnetoresistance and the I_{dc} induced GMR in the 2DES and whether possible mutual influence can be utilized to obtain new physical insight into the two effects. Thus, we examined the overlap of microwave photo-excited magnetoresistance oscillations[1–14,16–19,21,22,24,25,28–30,33–38] with a I_{dc}-induced positive and negative-GMR in the GaAs/AlGaAs 2DES[77,79–81]. The aims of this study were (a) to separate, if possible, the two effects when they occur together, using an empirically established multi-term Drude conduction model[77,80], in order to extract the characteristics of each individual effect, and (b) to then evaluate and determine possible mutual influence between the two effects. The results confirm separability of the two effects and show, in addition, that the GMR inducing I_{dc} serves to suppress the peaks (maxima) in the photo-excited magnetoresistance oscillations while leaving the valleys (minima) of the microwave induced oscillations relatively unaffected.

Results

Figure 1(a,b) exhibit the magnetoresistance of a GaAs/AlGaAs Hall bar specimen under $f = 70.1\ GHz$ photoexcitation at $T = 1.7\ K$. Figure 1(a) shows the diagonal resistance R_{xx} vs. the magnetic field, B, for various microwave source power levels, P. The non-oscillatory portion of the data show initial negative magnetoresistance to $B = 0.15\ T$, followed by positive magnetoresistance to $B = 0.35\ T$, with observable Shubnikov-de Haas oscillations

[1]Department of Physics and Astronomy, Georgia State University, Atlanta, Georgia, 30303, USA. [2]Laboratorium für Festkörperphysik, ETH Zürich, CH-8093, Zürich, Switzerland. Correspondence and requests for materials should be addressed to R.G.M. (email: rmani@gsu.edu)

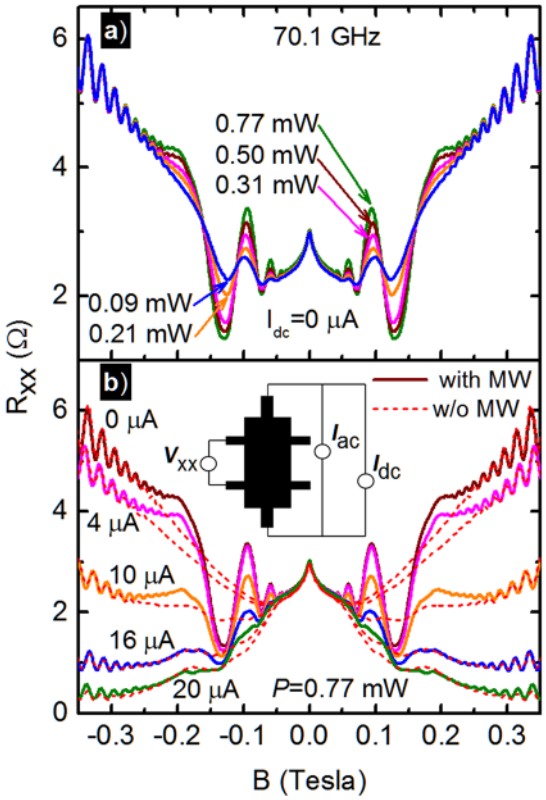

Figure 1. Radiation induced magnetoresistance oscillations in R_{xx} in a GaAs/AlGaAs hetreostructure 2D electron system. (**a**) R_{xx} is exhibited vs. the magnetic field, B, at different microwave power, P, for $0.09 \leq P \leq 0.77\, mW$ and $I_{dc} = 0\, \mu A$. (**b**) This panel exhibits R_{xx} vs. B, at different I_{dc} for $0 \leq I_{dc} \leq 20\, \mu A$, with microwave excitation at $f = 70.1$ GHz and $P = 0.77\, mW$ (solid lines), and under dark conditions (dashed lines).

for $B \geq 0.2\, T$[25,28]. The data also confirm, that in the standard photo-excited experiment, the radiation-induced magnetoresistance oscillations, which are observed roughly over the interval $-0.2 \leq B \leq 0.2\, T$, increase in amplitude with increasing P upto $P = 0.77\, mW$. The inset of Fig. 1(b) illustrates the configuration, which is the principal focus of this study, for the transport measurements carried out with a supplementary dc-current, I_{dc} in order to examine the influence of the I_{dc}[80] on both the non-oscillatory- and photo-excited oscillatory magnetoresistance in this system. Thus, the main panel of Fig. 1(b) exhibits the R_{xx} under constant photo-excitation of $f = 70.1\, GHz$ at $P = 0.77\, mW$ (solid lines) and in the dark (red-dashed-lines) for various values of I_{dc} over the span $0 \leq I_{dc} \leq 20\, \mu A$. A detailed study of the influence of I_{dc} on R_{xx} under dark conditions appears elsewhere[80]. Figure 1(b) shows that the non-oscillatory magnetoresistance below $B = 0.05\, T$ is uninfluenced by the I_{dc} while the magnetoresistance for $0.05 \leq B \leq 0.35\, T$ changes from an overall positive magnetoresistance to an overall negative giant magnetoresistance with increasing I_{dc}. That is, a negative magnetoresistance effect develops with increasing I_{dc} at $B \geq 0.05\, T$, which reduces the R_{xx} by nearly 40 percent at $0.10\, T$. Note that the $|B| \leq 0.05\, T$ magnetoresistance, which is unaffected by both P and I_{dc}, appears similar in shape to the weak-localization effect[77,78]. The figure also shows clearly that the amplitude of the photo-excited magnetoresistance oscillations decreases with increasing I_{dc}.

Since one aim of the study was to characterize the change in the radiation-induced magnetoresistance oscillations produced by the supplementary I_{dc} in order to gain further understanding of the physical effect of the I_{dc}, we worked to separate out the non-oscillatory and oscillatory terms in the observed R_{xx}. Thus, we introduced a fitting model that addressed both the weak localization like- and the "bell shape" giant magnetoresistance- terms. The weak localization like magnetoresistance was accounted for by including a term $R_{xx} = A\, ln(B_0/B)$, which is what would be expected from 2D WL theory upon neglecting spin-orbit and spin scattering[82,83]. The GMR effect was addressed with the multi-conduction Drude model[77]. Thus, we set $R_{xx} = \rho_{xx}(L/W)$, where, ρ_{xx} is the diagonal resistivity, and L/W is device length-to-width ratio. For the sample studied, $L/W = 1$, which sets $R_{xx} = \rho_{xx}$. The diagonal resistivity, ρ_{xx} and off-diagonal resistivity, ρ_{xy} were expressed in terms of diagonal conductivity, σ_{xx} and off-diagonal conductivity, σ_{xy} by $\rho_{xx} = \sigma_{xx}/\left[\sigma_{xx}^2 + \sigma_{xy}^2\right]$ and $\rho_{xy} = \sigma_{xy}/\left[\sigma_{xx}^2 + \sigma_{xy}^2\right]$. Since the experimental results indicate that the GMR changes with I_{dc}, see Fig. 1(b), the conductivities include two terms: $\sigma_{xx} = \sigma_{xx}^0 + \sigma_{xx}^1 = \sigma_0/[1 + (\mu_0 B)^2] + \sigma_1/[1 + (\mu_1 B)^2]$. (Similarly, $\sigma_{xy} = \sigma_{xy}^0 + \sigma_{xy}^1 = \mu_0\sigma_0 B/[1 + (\mu_0 B)^2] + \mu_1\sigma_1 B/[1 + (\mu_1 B)^2]$). The terms σ_{xx}^1 and σ_{xy}^1 account for the changes in the conductivity due I_{dc} and P. Note that $\sigma_{xy}^1 = \sigma_{xx}^1 \times \mu_1 B$. The zeroth conductivity terms, σ_{xx}^0 and σ_{xy}^0 represents the high mobility electrons in 2D-electron system. Thus, $\sigma_0 = n_0 e\mu_0$, where n_0 is the electron density and μ_0 is the electron mobility in the 2D electron system. The multi-conduction model with two conductivity terms includes four parameters μ_0, σ_0, μ_1 and σ_1. However,

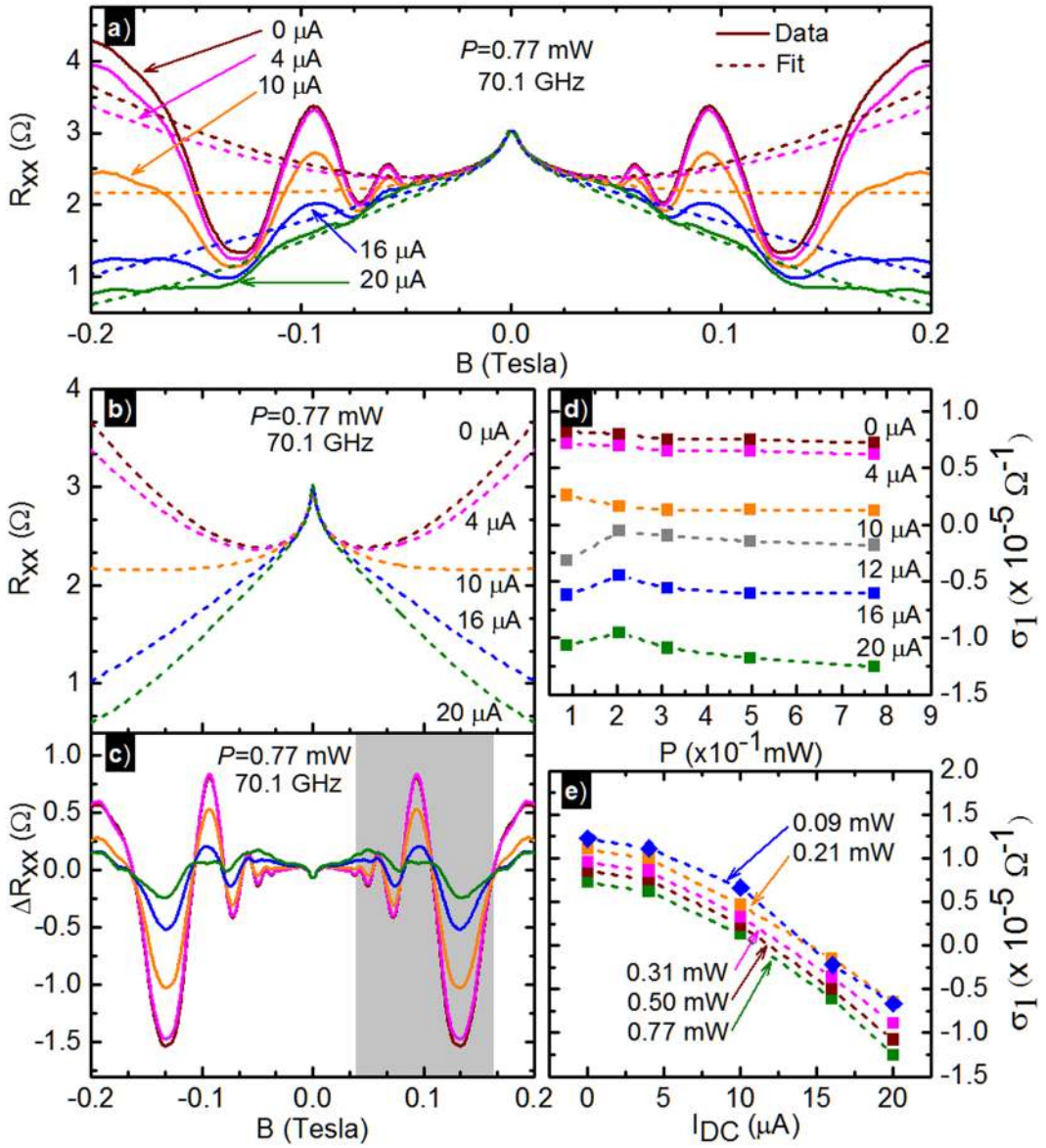

Figure 2. (**a**) Experimental data of Fig. 1(b) with model fits of the non-oscillatory giant magnetoresistance in the GaAs/AlGaAs 2DES using the multi-conduction model described in the text. (**b**) Fit extracted non-oscillatory R_{xx} of panel (a) at various dc-current, I_{dc} at $P = 0.77\,mW$. (**c**) This panel exhibits the extracted radiation-induced magnetoresistance oscillations after subtracting the model fits from the experimental data of panel (a), at various I_{dc} at $P = 0.77\,mW$. The highlighted region was used for the fits shown in Figs 3(a) and 4(a). (**d**) Model extracted conductivity σ_1 vs. P, at various I_{dc}. (**e**) Shows σ_1 vs. I_{dc} at different P, the traces are offset vertically by $1 \times 10^{-6}\,\Omega^{-1}$ for clarity. Dashed lines in (**d**,**e**) are guides to the eye.

the number of free parameters has been reduced to two, i.e. μ_1 and σ_1, by holding constant n_0 and μ_0 to the values extracted from the low field dark measurements at $I_{dc} = 0$. With such accounting for both the weak localization-like magnetoresistance and the bell-shape giant magnetoresistance, the experimental magnetoresistance data were fit to $R_{xx} = A\,ln(B_0/B) + \sigma_{xx}/[\sigma_{xx}^2 + \sigma_{xy}^2]$.

Figure 2(a) exhibits model fits of the non-oscillatory portion of the magnetoresistance data at different I_{dc}, under photoexcitation at $f = 70.1\,GHz$ and $P = 0.77\,mW$. Figure 2(b) shows the fit extracted non-oscillatory magnetoresistance. Figure 2(c) exhibits the residual resistance ΔR_{xx} after subtracting the best fit non-oscillatory magnetoresistance from the experimental data, i.e., $\Delta R_{xx} = R_{xx} - [A\,ln(B_0/B) + \sigma_{xx}/[\sigma_{xx}^2 + \sigma_{xy}^2]]$. Table 1 summarizes fitting parameters for the fits shown in Fig. 2(a,b). For a given I_{dc}, the non-oscillatory magnetoresistance can be fit with a constant μ_1 over the entire P-range. Figure 2(d,e) exhibit the fit extracted σ_1, which captures the behavior of the non-oscillatory giant magnetoresistance in the experimental data. As observable in Fig. 2(d), the σ_1 is not significantly affected by the applied P. In contrast, in Fig. 2(e), the σ_1 shows a large change as a function of I_{dc}. One can observe a clear transition of σ_1 from positive- to negative- values with increasing dc-bias from 0 μA to 20 μA. The sign-change in σ_1 occurs in the range of $10 \leq I_{dc} \leq 12\,\mu A$. Figure 1(b) suggests

I_{dc} (μA)	n_0 ($10^{11}\ cm^{-2}$)	μ_0 ($10^6\ cm^2/Vs$)	μ_1 ($10^6\ cm^2/Vs$)
0	2.4	11.4	0.019
4	2.4	11.4	0.021
8	2.4	11.4	0.036
12	2.4	11.4	0.041
16	2.4	11.4	0.045
20	2.4	11.4	0.062

Table 1. Parameters extracted from fits of non-oscillatory giant magnetoresistance in Fig. 2(a) at various I_{dc}, see text. Parameters n_0, μ_0 and μ_1 were held constant as a function of P at each I_{dc}. The parameter σ_1 has been plotted in Fig. 2(d,e).

that the crossover from positive- to negative- magnetoresistance, if one neglects the weak localization like term, occurs over roughly this I_{dc} interval.

Figure 3(a) exhibits the experimental oscillatory resistance, ΔR_{xx} in the range of $0.04 \leq B \leq 0.16\ T$ as symbols vs. the normalized inverse magnetic field scale FB^{-1}, where F is the magnetoresistance oscillation frequency, for different P and $I_{dc} = 0$. The ΔR_{xx} is obtained by subtracting the fit for the non-oscillatory magnetoresistance from the experimental data, as mentioned above. The plot indicates that the oscillatory extrema are shifted by 1/4 unit with respect to integral values on the abscissa scale, confirming a "1/4-cycle" phase shift in the radiation-induced magnetoresistance oscillations[3]. Further, in Fig. 3(a), the height of the oscillatory magnetoresistance peak indicated by the arrow (↑) decreases by ≈80 percent upon reducing the P by a factor of eight. The solid lines in red shown in the Fig. 3(a) are the nonlinear least square fits to the data using exponentially damped sinusoids, i.e., $\Delta R^{fit} = -A\exp(-\lambda/B)\sin(2\pi F/B)$[3,5,12,15,25,28]. Here, A is the oscillatory amplitude, F is the magnetoresistance oscillation frequency and λ is the damping factor. The data fits serve to extract three parameters: A, F and λ[3,5,12,25,28]. Since F is independent of the radiation-intensity it was fixed to a constant value[25]. The fit indicates $F = 0.1610\ T$ at $f = 70.1\ GHz$, which suggests that $m^*/m = eF/(2\pi mf) = 0.064$, slightly lower than the standard value, $m^*/m = 0.067$ for GaAs/AlGaAs 2DES system. Figure 3(b) shows the oscillatory magnetoresistance amplitude, A vs. P for different I_{dc} (circles), along with a fit of the results to $A = A_0P^{\beta}$. Here, the oscillatory resistance amplitude shows a sub-linear growth with increasing P, as reported previously. The fit extracted A_0 and β are summarized in the Table 2. The table shows that β decreases with increasing I_{dc}, a consequence of the fact that the oscillations get smaller with increasing I_{dc}[25,54]. Finally, Fig. 3(c) shows the fit extracted oscillation damping factor, λ, vs. P. Here, $\lambda = 0.234 \pm 0.003$ served to fit the entire P range.

The highlighted oscillatory resistances in Fig. 2(c) have been fit to exponentially damped sinusoids. Figure 4(a) shows ΔR_{xx} vs. the normalized inverse magnetic field scale FB^{-1}, where F is the magnetoresistance oscillation frequency, for different I_{dc} and $P = 0.77\ mW$, along with data fits to the exponentially damped sinusoids mentioned above. Figure 4(a) shows that the radiation-induced magnetoresistance oscillations are gradually reduced in amplitude with increasing I_{dc}. However, the extrema remain mostly unshifted with increasing I_{dc}. Figure 4(b) show the extracted oscillatory amplitude A vs. I_{dc} at different microwave power levels P. From the plot, it is clear that the A decreases with I_{dc} at each P. Figure 4(c) shows that a constant damping factor λ serves to fit the ΔR_{xx} for $0 \leq I_{dc} \leq 20\ \mu A$.

Discussion

Our recent work has examined a current-tunable giant magnetoresistance in the GaAs/AlGaAs 2D system[80]. This work aimed to study possible interplay between radiation-induced magnetoresistance oscillations and the dc-current induced non-oscillatory giant magnetoresistance, in order to further understand any possible mutual influence between these two effects. Thus, systematic measurements of the R_{xx} were carried out as a function of both the microwave power P (at a constant microwave frequency f), and the supplemental dc current I_{dc}.

As a function of P at $I_{dc} = 0\ \mu A$, the canonical "1/4-cycle" shifted radiation-induced oscillations were observed (Fig. 1(a)), the oscillations could be fit with exponentially damped sinusoids (Fig. 3(a)), the oscillatory amplitude increased non-linearly with P (Fig. 3(b)), and the damping factor λ remained unchanged with P (Fig. 3(c))[1,3,5–14,16–19,21,22,24–26,28–30,34,35,37,38].

As a function of I_{dc} at a fixed P, the progresssive increase of I_{dc} revealed a systematic change in the non-oscillatory giant magnetoresistance (Fig. 1(b)). This nonoscillatory giant magnetoresistance could be successfully fit with a two term Drude model (Fig. 2(a,b))[77]. The fit parameter σ_1 tracked the change in the non-oscillatory magnetoresistance with I_{dc}, see Fig. 2(e). The results show that σ_1 decreases with increasing I_{dc}, sign reversal is observable in σ_1, and the sign reversal correlates with a change from overall positive to overall negative magnetoresistance (cf. Fig. 2(a,e)). Such fits also show that although the non-oscillatory giant magnetoresistance is sensitive to I_{dc}, it is not as sensitive to the microwave power P. This latter feature is reflected in the relative invariance of σ_1 vs. P, see Fig. 2(d).

As a function of I_{dc} at fixed P, the progressive increase of I_{dc} also serves to reduce the amplitude of the radiation-induced magnetoresistance oscillations, see Figs 1(b), 2(a,c) and 4(a). For each I_{dc}, the magnetoresistance oscillations at a fixed P could be fit with exponentially damped sinusoids, with a constant damping factor λ, see Fig. 4(a,c). The magnetoresistance oscillation amplitude dropped monotonically with increasing I_{dc} at each microwave power P, see Fig. 4(b).

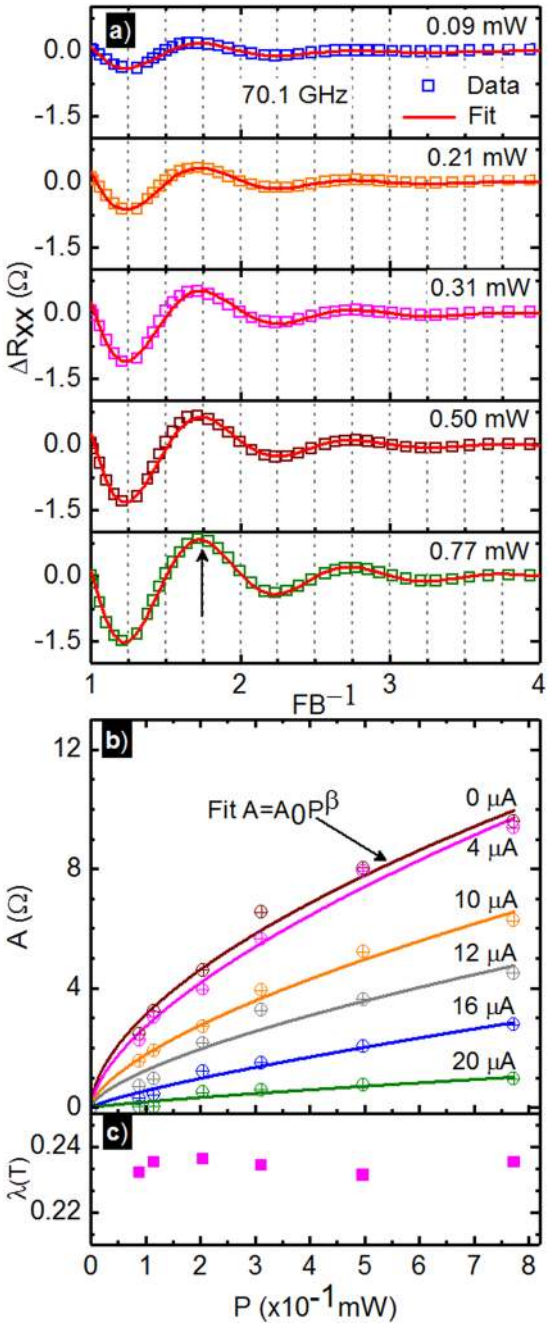

Figure 3. (**a**) This figure exhibits the oscillatory ΔR_{xx} extracted by subtracting the non-oscillatory magnetoresistance from the experimental data at different microwave power. The plot shows ΔR_{xx} vs. FB^{-1} at various P for $I_{dc} = 0\,\mu A$. Here, F is the magnetoresistance oscillation frequency and B is the magnetic field. The symbols represent data while the lines represent fits to exponentially damped sinusoids, see text. (**b**) The magnetoresistance oscillation amplitude, A, vs. P is shown for different I_{dc} from $0\,\mu A$ to $20\,\mu A$ (circles). Also shown are the power-law fits, $A = A_0 P^{\beta}$ (solid lines). Fit extracted A_0 and β are shown in Table 2. (c) The damping constant, λ, in the exponentially damped sinusoidal fit of the oscillatory magnetoresistance is plotted vs. P.

This work therefore shows that the I_{dc} tunable giant magnetoresistance in the GaAs/AlGaAs 2D system follows the multiconduction Drude model even when supplementary radiation-induced magnetoresistance oscillations are induced by microwave photo-excitation of the specimen. Indeed, the radiation-induced magnetoresistance oscillations and the giant magnetoresistance appear separable in the sense that one may fit the non-oscillatory magnetoresistance, proceeding as though the magnetoresistance oscillations do not exist, and remove it from the experimental data, to obtain separated giant magnetoresistance and radiation-induced magnetoresistance oscillations. At the moment, the only observable mutual influence appears to be the reduction in the amplitude of the radiation-induced magnetoresistance oscillations with increased I_{dc}.

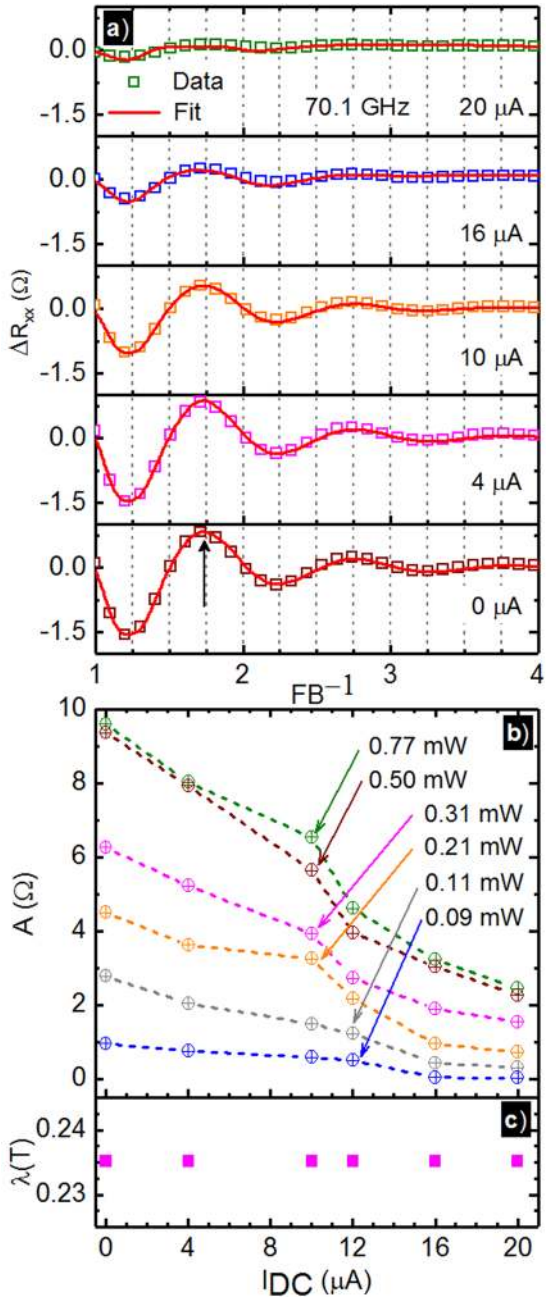

Figure 4. (**a**) This figure exhibits the oscillatory ΔR_{xx} extracted by subtracting the non-oscillatory magnetoresistance from the experimental data at different I_{dc}. The plot shows ΔR_{xx} vs. FB^{-1} at various $I_{dc} = 0\,\mu A$ for $P = 0.77\,mW$. Here, F is the magnetoresistance oscillation frequency and B is the magnetic field. The symbols represent data while the lines represent fits to exponentially damped sinusoids, see text. (**b**) The fit extracted magnetoresistance oscillation amplitude, A, vs. I_{dc} is shown for different P from $0.09\,mW$ to $0.77\,mW$ (circles). The dashed lines are guides to the eye. (**c**) The damping constant, λ, in the exponentially damped sinusoidal fit of the oscillatory magnetoresistance is plotted vs. I_{dc}.

A close examination of Fig. 1(b) shows that the reduction in the amplitude of the radiation-induced magnetoresistance oscillations with increasing I_{dc} proceeds in a curiously asymmetric manner: Increasing I_{dc} greatly reduces the R_{xx} at the oscillatory maxima while the effect of the I_{dc} on the R_{xx} minima is much smaller. This feature suggests one possible route to understanding the results: In the strong field condition, $\omega\tau \gg 1$, which is satisfied at $B \geq 0.001\,T$ in such specimens, the ρ_{xx} is directly proportional to the σ_{xx}, i.e., $\rho_{xx} \propto \sigma_{xx}/\sigma_{xy}^2$. This implies that reduced diagonal resistance/resistivity is a consequence of reduced diagonal conductance/conductivity. Thus, one might say that at the oscillatory resistance maxima, the diagonal conductivity is suppressed with increasing I_{dc} in Fig. 1(b). On the other hand, at the minima, see Fig. 1(b), the relative insensitivity of R_{xx} to the I_{dc} indicates that the diagonal conductivity cannot suppressed further by the I_{dc}. One way to understand this feature is to assert that 'optimal' microwave photo-excitation reduces the diagonal conductivity to its lowest possible value at the

I_{dc} (μA)	A (Ω)	β.
0	11.5	0.57
4	11.4	0.62
8	7.7	0.64
12	5.6	0.66
16	3.5	0.79
20	1.5	0.81

Table 2. Fit parameters obtained for power law fits, see Fig. 3(b), of the amplitude of the oscillatory magnetoresistance induced by photo-excitation at different I_{dc}.

oscillatory minima at a given temperature, and that the I_{dc} is not very effective in reducing the diagonal conductivity further, below this value. As a consequence, I_{dc} fails to make a significant change at the oscillatory magnetoresistance minima. On the other hand, at the photo-excited oscillatory magnetoresistance maxima, where photo-excitation serves to enhance the diagonal conductivity above the dark value, the supplemental current can be very effective in reducing the conductivity because there is room to do so and, therefore, the diagonal resistance at the oscillatory maxima is suppressed by the I_{dc}. When, at say $I_{dc} = 20\ \mu A$ in Fig. 1(b), I_{dc} has its optimal effect, the radiation-induced magnetoresistance oscillations disappear mostly because the supplemental current prevents the oscillatory resistance (conductance) enhancements that occur at the peaks of the radiation-induced magnetoresistance oscillations.

Finally, we note here that prior work by Hatke and co-workers[73] examined the effect of the dc-drive at cyclotron resonance subharmonics at $f = 27$ GHz. In comparison, we examine the effect of dc-drive at cyclotron resonance harmonics at $f = 70.1$ GHz. Cyclotron resonance subharmonics are not evident at $f = 70.1\ GHz$. Bykov *et al.*[72] examined the effect of a dc-drive without microwaves in strong magnetic fields with strong Shubnikov de Haas oscillations, while this work examines the interplay between the dc-drive and the microwave excitation on the magnetotransport.

Conclusions

In summary, this study shows that a I_{dc} tunable giant magnetoresistance can coexist with radiation-induced magnetoresistance oscillations in the GaAs/AlGaAs 2D electron system. Further, the two effects are separable and can be separated using a two term Drude multi-conduction model. It appears that the radiation-induced magnetoresistance oscillations have a minimal effect on the current-tunable non-oscillatory magnetoresistance. On the other hand the I_{dc} responsible for the magnetoresistance produces a progressive and rather asymmetric decrease in the amplitude of the radiation-induced oscillations. The results suggest that the supplemental I_{dc} serves to produce an overall decrease in the diagonal conductivity, and this serves to reduce and eventually eliminate the conductivity enhancements at the peaks of the radiation-induced oscillatory magnetoresistance. Since dissipative transport in the strong field magnetic limit proceeds by scattering from state to state in the vicinity of the Fermi level, it appears that the I_{dc} serves to suppress such scattering in the strong field limit.

Methods

High mobility MBE GaAs/AlGaAs heterostructures were patterned into Hall bars by photolithography. Four terminal electrical measurements were carried out on the Hall bars using low frequency lock-in based techniques with the sample mounted at the end of a cylindrical waveguide, within a variable temperature insert, inside a superconducting solenoid in the $B \perp I$ configuration. Since the 200 μm wide Hall bars included voltage probes spaced by 200 μm, the effective Length-to-Width (L/W) ratio for the measurements presented here is L/W = 1. The samples were photo-excited via a cylindrical waveguide and the incident power was systematically varied using variable attenuators. The samples were immersed in liquid helium and temperature control was realized by controlling the vapor pressure of liquid helium. The ac- and dc- currents were applied as shown in the inset of Fig. 1(b). The lock-in sourced ac current source was held constant, as a dc current was varied as desired under computer control, at a series of microwave power levels P. Typically, magnetic field (B) sweeps of the lock-in detected diagonal voltage V_{xx} were collected at a fixed temperature, T, in order to determine $R_{xx} = V_{xx}/I_{ac}$.

References

1. Mani, R. G. *et al.* Zero-resistance states induced by electromagnetic wave excitation in GaAs/AlGaAs heterostructures. *Nature* **420**, 646–650 (2002).
2. Zudov, M. A., Du, R. R., Pfeiffer, L. N. & West, K. W. Evidence for a new dissipationless effect in 2D electronic transport. *Phys. Rev. Lett.* **90**, 046807-1-4 (2003).
3. Mani, R. G. *et al.* Demonstration of a 1/4 cycle phase shift in the radiation-induced oscillatory-magnetoresistance in GaAs/AlGaAs devices. *Phys. Rev. Lett.* **92**, 146801-1-4 (2004).
4. Kovalev, A. E., Zvyagin, S. A., Bowers, C. R., Reno, J. L. & Simmons, J. A. Observation of a node in the quantum oscillations induced by microwave radiation. *Sol. St. Comm.* **130**, 379–381 (2004).
5. Mani, R. G. *et al.* Radiation induced oscillatory Hall effect in high mobility GaAs/AlGaAs devices. *Phys. Rev. B* **69**, 161306-1-4 (2004).
6. Mani, R. G. *et al.* Radiation induced zero-resistance states in GaAs/AlGaAs heterostructures: Voltage-current characteristics and intensity dependence at the resistance minima. *Phys. Rev. B* **70**, 155310-1-5 (2004).
7. Mani, R. G. *et al.* Radiation-induced oscillatory magnetoresistance as a sensitive probe of the zero-field spin splitting in high-mobility GaAs/AlGaAs devices. *Phys. Rev. B* **69**, 193304-1-4 (2004).
8. Mani, R. G. Zero-resistance states induced by electromagnetic-wave excitation in GaAs/AlGaAs heterostructures. *Physica E (Amsterdam)* **22**, 1–6 (2004).

9. Du, R. R., Zudov, M. A., Yang, C. L., Pfeiffer, L. N. & West, K. W. Dissipationless 2D electronic transport induced by microwaves. *Physica E* **22**, 7–12 (2004).
10. Mani, R. G. Radiation-induced zero-resistance states with resolved Landau levels. *Appl. Phys. Lett.* **85**, 4962–4964 (2004).
11. Simovic, B., Ellenberger, C., Ensslin, K. & Wegscheider, W. Density dependence of microwave induced magnetoresistance oscillations in a two-dimensional electron gas. *Phys. Rev. B* **71**, 233303-1-4 (2005).
12. Mani, R. G. Radiation-induced oscillatory magnetoresistance in a tilted magnetic field in GaAs/AlGaAs devices. *Phys. Rev. B* **72**, 075327-1-5 (2005).
13. Mani, R. G. Photo-excited zero-resistance states in quasi-two-dimensional GaAs/AlGaAs devices. *Sol. St. Comm.* **144**, 409–412 (2004).
14. Smet, J. H. *et al*. Circular-polarization-dependent study of the microwave photoconductivity in a two-dimensional electron system. *Phys. Rev. Lett.* **95**, 116804-1-4 (2005).
15. Mani, R. G. Spin characterization and control over the regime of the radiation-induced zero-resistance states. *IEEE Trans. Nanotechnol.* **4**, 27–34 (2005).
16. Mani, R. G. Radiation-induced decay of Shubnikov-de Haas oscillations in the regime of the radiation-induced zero-resistance states. *Appl. Phys. Lett.* **91**, 132103-1-3 (2007).
17. Wirthmann, A. *et al*. Far-infrared-induced magnetoresistance oscillations in GaAs/AlGaAs-based two-dimensional electron systems. *Phys. Rev. B* **76**, 195315-1-5 (2007).
18. Studenikin, S. A. *et al*. Frequency quenching of microwave-induced resistance oscillations in a high-mobility two-dimensional electron gas. *Phys. Rev. B* **76**, 165321-1-6 (2007).
19. Mani, R. G. Narrow-band radiation-sensing in the Terahertz and microwave bands using the radiation-induced magnetoresistance oscillations. *Appl. Phys. Lett.* **92**, 102107-1-3 (2008).
20. Wiedmann, S. *et al*. Interference oscillations of microwave photoresistance in double quantum wells. *Phys. Rev. B* **78**, 121301-1-4 (2008).
21. Mani, R. G., Johnson, W. B., Umansky, V., Narayanamurti, V. & Ploog, K. Phase study of oscillatory resistances in microwave irradiated and dark GaAs/AlGaAs devices: Indications of an unfamiliar class of integral quantum Hall effect. *Phys. Rev. B* **79**, 205320-1-10 (2009).
22. Chepelianskii, A. D. & Shepelyansky, D. L. Microwave stabilization of edge transport and zero-resistance states. *Phys. Rev. B* **80**, 241308-1-4 (2009).
23. Wiedmann, S. *et al*. Magnetoresistance oscillations in multilayer systems: Triple quantum wells. *Phys. Rev. B* **80**, 245306-1-9 (2009).
24. Konstantinov, D. & Kono, K. Photon-induced vanishing of magnetoconductance in 2D electrons on liquid helium. *Phys. Rev. Lett.* **105**, 226801-1-4 (2010).
25. Mani, R. G., Gerl, C., Schmult, S., Wegscheider, W. & Umansky, V. Nonlinear growth with the microwave intensity in the radiation-induced magnetoresistance oscillations. *Phys. Rev. B* **81**, 125320-1-6 (2010).
26. Wiedmann, S., Gusev, G. M., Raichev, O. E., Bakarov, A. K. & Portal, J. C. Thermally activated intersubband scattering and oscillating magnetoresistance in quantum wells. *Phys. Rev. B* **82**, 165333-1-8 (2010).
27. Wiedmann, S., Gusev, G. M., Raichev, O. E., Bakarov, A. K. & Portal, J. C. Microwave zero-resistance states in a bilayer electron system. *Phys. Rev. Lett.* **105**, 026804-1-4 (2010).
28. Ramanayaka, A. N., Mani, R. G. & Wegscheider, W. Microwave induced electron heating in the regime of the radiation-induced magnetoresistance oscillations. *Phys. Rev. B* **83**, 165303-1-5 (2011).
29. Mani, R. G., Ramanayaka, A. N. & Wegscheider, W. Observation of linear-polarization-sensitivity in the microwave-radiation-induced magnetoresistance oscillations. *Phys. Rev. B* **84**, 085308-1-4 (2011).
30. Ramanayaka, A. N., Mani, R. G., Inarrea, J. & Wegscheider, W. Effect of rotation of the polarization of linearly polarized microwaves on the radiation-induced magnetoresistance oscillations. *Phys. Rev. B* **85**, 205315-1-6 (2012).
31. Mani, R. G., Hankinson, J., Berger, C. & de Heer, W. A. Observation of resistively detected hole spin resonance and zero-field pseudo-spin splitting in graphene. *Nature Commun.* **3**, 996, doi:10.1038/ncomms1986 (2012).
32. Konstantinov, D., Monarkha, Y. & Kono, K. Effect of coulomb interaction on microwave-induced magnetoconductivity oscillations of surface electrons on liquid helium. *Phys. Rev. Lett.* **111**, 266802-1-5 (2013).
33. Mani, R. G., Kriisa, A. & Wegscheider, W. Magneto-transport characteristics of a 2D electron system driven to negative magneto-conductivity by microwave photoexcitation. *Sci. Rep.* **3**, 3478, doi:10.1038/srep03478 (2013).
34. Mani, R. G. *et al*. Terahertz photovoltaic detection of cyclotron resonance in the regime of the radiation-induced magnetoresistance oscillations. *Phys.Rev. B* **87**, 245308-1-8 (2013).
35. Ye, T., Liu, H.-C., Wegscheider, W. & Mani, R. G. Combined study of microwave-power/linear polarization dependence of the microwave-radiation-induced magnetoresistance oscillations in GaAs/AlGaAs devices. *Phys. Rev. B* **89**, 155307-1-5 (2014).
36. Chepelianskii, A. D., Watanabe, N., Nasyedkin, K., Kono, K. & Konstantinov, D. An incompressible state of a photo-excited electron gas. *Nat. Comm.* **6**, 7210, doi:10.1038/ncomms8210 (2015).
37. Ye, T., Liu, H.-C., Wang, Z., Wegscheider, W. & Mani, R. G. Comparative study of microwave radiation-induced magnetoresistive oscillations induced by circularly- and linearly- polarized photoexcitation. *Sci. Rep.* **5**, 14880, doi:10.1038/srep14880 (2015).
38. Herrmann, T. *et al*. Analog of microwave-induced resistance oscillations induced in GaAs heterostructures by terahertz radiation. *Phys. Rev. B* **94**, 081301-1-5 (2016).
39. Liu, H.-C., Samaraweera, R. L., Reichl, C., Wegscheider, W. & Mani, R. G. Study of the angular phase shift in the polarization angle dependence of the microwave induced magnetoresistance oscillations. *Phys. Rev. B* **94**, 245312-1-7 (2016).
40. Durst, A. C., Sachdev, S., Read, N. & Girvin, S. M. Radiation-induced magnetoresistance oscillations in a 2D electron gas. *Phys. Rev. Lett.* **91**, 086803-1-4 (2003).
41. Ryzhii, V. & Suris, R. Nonlinear effects in microwave photoconductivity of two-dimensional electron systems. *J. Phys.: Cond. Matt.* **15**, 6855–6869 (2003).
42. Andreev, A. V., Aleiner, I. L. & Millis, A. J. Dynamical symmetry breaking as the origin of the zero-dc-resistance state in an ac-driven system. *Phys. Rev. Lett.* **91**, 056803-1-4 (2003).
43. Koulakov, A. A. & Raikh, M. E. Classical model for the negative dc conductivity of ac-driven two-dimensional electrons near the cyclotron resonance. *Phys. Rev. B* **68**, 115324-1-4 (2003).
44. Lei, X. L. & Liu, S. Y. Radiation-induced magnetoresistance oscillation in a two-dimensional electron gas in Faraday geometry. *Phys. Rev. Lett.* **91**, 226805-1-4 (2003).
45. Rivera, P. H. & Schulz, P. A. Radiation-induced zero-resistance states: Possible dressed electronic structure effects. *Phys. Rev. B* **70**, 075314-1-6 (2004).
46. Dmitriev, I. A., Vavilov, M. G., Aleiner, I. L., Mirlin, A. D. & Polyakov, D. G. Theory of microwave-induced oscillations in the magnetoconductivity of a two-dimensional electron gas. *Phys. Rev. B* **71**, 115316-1-11 (2005).
47. Torres, M. & Kunold, A. Kubo formula for Floquet states and photoconductivity oscillations in a two-dimensional electron gas. *Phys. Rev. B* **71**, 115313-1-13 (2005).
48. Lei, X. L. & Liu, S. Y. Radiation-induced magnetotransport in high mobility two-dimensional systems: Role of electron heating. *Phys. Rev. B* **72**, 075345-1-10 (2005).
49. Inarrea, J. & Platero, G. Theoretical approach to microwave radiation-induced zero-resistance states in 2D electron systems. *Phys. Rev. Lett.* **94**, 016806-1-4 (2005).

50. Inarrea, J. & Platero, G. Temperature effects on microwave-induced resistivity oscillations and zero-resistance states in two-dimensional electron systems. *Phys. Rev. B* **72**, 193414-1-4 (2005).
51. Raichev, O. E. Magnetic oscillations of resistivity and absorption of radiation in quantum wells with two populated subbands. *Phys. Rev. B* **78**, 125304-1-14 (2008).
52. Inarrea, J. Effect of frequency and temperature on microwave-induced magnetoresistance oscillations in two-dimensional electron systems. *Appl. Phys. lett.* **92**, 192113-1-3 (2008).
53. Dmitriev, I. A., Khodas, M., Mirlin, A. D., Polyakov, D. G. & Vavilov, M. G. Mechanisms of the microwave photoconductivity in two-dimensional electron systems with mixed disorder. *Phys. Rev. B* **80**, 165327-1-9 (2009).
54. Inarrea, J., Mani, R. G. & Wegscheider, W. Sublinear radiation power dependence of photoexcited resistance oscillations in two-dimensional electron systems. *Phys. Rev. B* **82**, 205321-1-5 (2010).
55. Mikhailov, S. A. Theory of microwave-induced zero-resistance states in two-dimensional electron systems. *Phys. Rev. B* **83**, 155303-1-12 (2011).
56. Inarrea, J. Influence of linearly polarized radiation on magnetoresistance in irradiated two-dimensional electron systems. *Appl. Phys. Lett.* **100**, 242103-1-3 (2012).
57. Lei X. L. & Liu, S. Y. Linear polarization dependence of microwave-induced magnetoresistance oscillations in high mobility two-dimensional systems. *Phys. Rev. B* **86**, 205303-1-5 (2012).
58. Iñarrea, J. Linear polarization sensitivity of magnetotransport in irradiated two-dimensional electron systems. *J. Appl. Phys.* **113**, 183717-1-5 (2013).
59. Zhirov, O. V., Chepelianskii, A. D. & Shepelyansky, D. L. Towards a synchronization theory of microwave-induced zero-resistance states. *Phys. Rev. B* **88**, 035410-1-14 (2013).
60. Raichev, O. E. Theory of magnetothermoelectric phenomena in high-mobility two-dimensional electron systems under microwave irradiation. *Phys. Rev. B* **91**, 235307-1-16 (2015).
61. Beltukov, Y. M. & Dyakonov, M. I. Microwave-induced resistance oscillations as a classical memory effect. *Phys. Rev. Lett.* **116**, 176801-1-5 (2016).
62. Chang, C.-C., Chen, G.-Y. & Lin, L. Dressed photon induced resistance oscillation and zero-resistance in arrayed simple harmonic oscillators with no impurity. *Sci. Rep.* **6**, 37763, doi:10.1038/srep37763 (2016).
63. Girvin, S. M., Jonson, M. & Lee, P. A. Interaction effects in disordered Landau-level systems in two dimensions. *Phys. Rev. B.* **26**, 1651–1659 (1982).
64. Houghton, A., Senna, J. R. & Ying, S. C. Magnetoresistance and Hall effect of a disordered interacting two-dimensional electron system. *Phys. Rev. B* **25**, 2196–2210 (1982).
65. Paalanen, M. A., Tsui, D. C. & Hwang, J. C. M. Parabolic Magnetoresistance from the Interaction Effect in a Two-Dimensional Electron Gas. *Phys. Rev. Lett.* **51**, 2226–2229 (1983).
66. Choi, K. K., Tsui, D. C. & Palmateer, S. C. Electron-electron interaction in GaAs-AlGaAs heterostructures. *Phys. Rev. B* **33**, 8216–8227 (1986).
67. Mani, R. G., von Klitzing, K. & Ploog, K. Magnetoresistance over the intermediate localization regime in GaAs/AlGaAs quantum wires. *Phys. Rev. B* **48**, 4571–4574 (1993).
68. Mani, R. G., von Klitzing, K. & Ploog, K. Localization at high magnetic fields in GaAs/AlGaAs quantum wires. *Phys. Rev. B* **15**, 9877–9880 (1992).
69. Mirlin, A. D., Polyakov, D. G., Evers, F. & Wolfle, P. Quasiclassical negative magnetoresistance of a 2D electron gas: Interplay of strong scatterers and smooth disorder. *Phys. Rev. Lett.* **87**, 126805-1-4 (2001).
70. Li, L., Proskuryakov, Y. Y., Savchenko, A. K., Linfield, E. H. & Ritchie, D. A. Magnetoresistance of a 2D electron gas caused by electron interactions in the transition from the diffusive to the ballistic regime. *Phys. Rev. Lett.* **90**, 076802-1-4 (2003).
71. Zhang, W., Zudov, M. A., Pfeiffer, L. N. & West, K. W. Resistance Oscillations in Two-Dimensional Electron Systems Induced by both ac and dc Fields. *Phys. Rev. Lett.* **98**, 106804-1-4 (2007).
72. Bykov, A. A., Zhang, J.-Q., Vitkalov, S., Kalagin, A. K. & Bakarov, A. K. Zero-differential resistance state of two-dimensional electron systems in strong magnetic fields. *Phys. Rev. Lett.* **99**, 116801-1-4 (2007).
73. Hatke, A. T., Chiang, H. S., Zudov, M. A., Pfeiffer, L. N. & West K. W. Microwave photoresistance in dc-driven 2D systems at cyclotron resonance subharmonics. *Phys. Rev. Lett.* **101**, 246811-1-4 (2008).
74. Inarrea, J. Interplay of dc current and microwaves in the magnetotransport of two-dimensional electron systems. *Phys. Rev. B* **80**, 193302-1-4 (2009).
75. Bockhorn, L., Barthold, P., Schuh, D., Wegscheider, W. & Haug, R. J. Magnetoresistance in a high mobility two-dimensional electron gas. *Phys. Rev. B* **83**, 113301-1-4 (2011).
76. Hatke, A. T., Zudov, M. A., Reno, J. L., Pfeiffer, L. N. & West, K. W. Giant negative magnetoresistance in high-mobility two-dimensional electron systems. *Phys. Rev. B* **85**, 081304-1-6 (2012).
77. Mani, R. G., Kriisa, A. & Wegscheider, W. Size-dependent giant-magnetoresistance in millimeter scale GaAs/AlGaAs 2D electron devices. *Sci. Rep.* **3**, 2747, doi:10.1038/srep02747 (2013).
78. Bockhorn, L. *et al.* Magnetoresistance induced by rare strong scatterers in a high-mobility two-dimensional electron gas. *Phys. Rev. B* **90**, 165434-1-5 (2014).
79. Inarrea, J. Theoretical model for negative giant magnetoresistance in ultra high mobility 2D electron systems. *Europhys. Lett.* **106**, 47005-1-5 (2014).
80. Wang, Z., Samaraweera, R. L., Reichl, C., Wegscheider, W. & Mani, R. G. Tunable electron heating induced giant magnetoresistance in the high mobility GaAs/AlGaAs 2D electron system. *Sci. Rep.* **6**, 38516, doi:10.1038/srep38516 (2016).
81. Inarrea, J., Bockhorn, L. & Haug, R. J. Negative huge magnetoresistance in high mobility 2D electron gases: DC-current dependence. *Europhys. Lett.* **115**, 17005-1-5 (2016).
82. Hikami, S., Larkin, A. I. & Nagaoka, Y. Spin-orbit interaction and magnetoresistance in the two-dimensional random system. *Prog. Theor. Phys.* **63**, 707–710 (1980).
83. Bergmann, G. Weak localization in thin films - a time-of-flight experiment with conduction electrons. *Phys. Repts.* **107**, 1–58 (1984).

Acknowledgements

This work was supported by the Army Research Office under W911NF-14-2-0076 and W911NF-15-1-0433 and the US Department of Energy, Office of Basic Energy Sciences, Material Science and Engineering Division under DE-SC0001762.

Author Contributions

Measurements were carried out by R.L.S. Technical support for cryogenic measurements was provided by H.-C. Liu. Z.W. contributed to the fitting discussions. Experimental development, data modeling, and manuscript by R.L.S. and R.G.M. High quality GaAs/AlGaAs wafers due to C.R. and W.W.

Additional Information

Competing Interests: The authors declare that they have no competing interests.

Publisher's note: Springer Nature remains neutral with regard to jurisdictional claims in published maps and institutional affiliations.